Concentration fields of the ternary systems and trajectory of phases in T-x-y Diagrams

V Lutsyk[1,2] **and A Zelenaya**[1]

[1] Institute of Physical Materials Science (Siberian Branch of Russian Academy of Sciences), Ulan-Ude, Russian Federation
[2] Buryat State University, Ulan-Ude, Russian Federation

E-mail: vluts@ipms.bscnet.ru

Abstract. The possibility of computer models of T-x-y diagrams for analysis two-, one- and zero-dimensional concentration fields are demonstrated using T-x-y diagram of systems CaO-SiO_2-Al_2O_3 and MgO-SiO_2-Al_2O_3. The characteristics of processes proceeding in the concentration fields can be analyzed with the help of diagrams of vertical mass balances, which show the increase or decrease of phases portions for each phase region. Calculation of crystallization paths was made.

1. Introduction

Construction of computer models of ternary systems significantly extends the possibilities of their investigation [1] by the calculation of crystallization paths and the analysis of concentration fields in order to obtain the information about the crystallization stages and the microconstituents. The schema of mono- and invariant equilibria is created on a basis of the data for invariant processes in the binary and ternary systems taking into account the existence and type of binary and ternary compounds. At the first stage of construction of 3D model for T-x-y diagrams, the invariant horizontal complexes at the temperatures of ternary points are reconstructed. Then they are completed by the ruled and unruled surfaces, and the phase regions are formed [2-4]. At the description of surfaces having a complex geometric structure (e.g. the large quantity of points on surface's contour, the presence of extremes or the gap of smoothness) we used the kinematic method based on the description of surfaces by means of the directing and forming curves [2-3, 5].

Systems CaO-SiO_2-Al_2O_3 and MgO-SiO_2-Al_2O_3 having a great practical importance are the objects of investigation. These systems are used at the description of properties of building materials [6-7] as well as at the characterization of geological objects [8-9].

2. Model of T-x-y diagrams of system CaO-SiO_2-Al_2O_3

The complexity of elaboration of T-x-y diagram model for system CaO-SiO_2-Al_2O_3 is associated with the ambiguous descriptions for binary systems, as well as the liquidus surfaces. There are different descriptions of types binary and ternary points, the character of binary compounds. The model of T-x-y diagram is based on the experimental data from [11]. It includes 16 liquidus surfaces and liquid immiscibility surface (fig. 1a), 128 ruled surfaces, 16 horizontal complexes at the temperatures of invariant points, 33 two-phase regions and 46 three-phase regions [4, 11-13].

Notations: incongruently melting compounds R_1 – $3CaO{\cdot}SiO_2$, R_3 – $3CaO{\cdot}2SiO_2$, R_6 – $3CaO{\cdot}Al_2O_3$, R_{10} – $CaO{\cdot}6Al_2O_3$; and congruently melting compounds R_2 – $2CaO{\cdot}SiO_2$, R_4 – $CaO{\cdot}SiO_2$, R_5 – $3Al_2O_3{\cdot}2SiO_2$, R_7 – $5CaO{\cdot}3Al_2O_3$, R_8 – $CaO{\cdot}Al_2O_3$, R_9 – $CaO{\cdot}2Al_2O_3$, R_{11} – $2CaO{\cdot}Al_2O_3{\cdot}SiO_2$, R_{12} – $CaO{\cdot}Al_2O_3{\cdot}2SiO_2$.

The most complex geometrical structure have the liquidus surfaces corresponding R_{11} and R_{12} with the contours $Q_4Q_5(Q_5,Q_6)Q_6E_6E_3(E_2,E_3)E_2Q_9$, $E_3(E_3,E_4)E_4(E_4,E_5)E_5Q_8(Q_7,Q_8)Q_7E_6$. There are maximum points on the monovariant liquidus lines E_2E_3, E_3E_4, E_4E_5, E_6E_3, Q_4Q_9, Q_5Q_6, Q_7Q_8 and inside surfaces due to the presence of ternary congruently melting compounds R_{11} and R_{12} (Fig. 1b-d). Such surfaces are constructed from several fragments with regards to the smoothness on boundaries of fragments [3, 5].

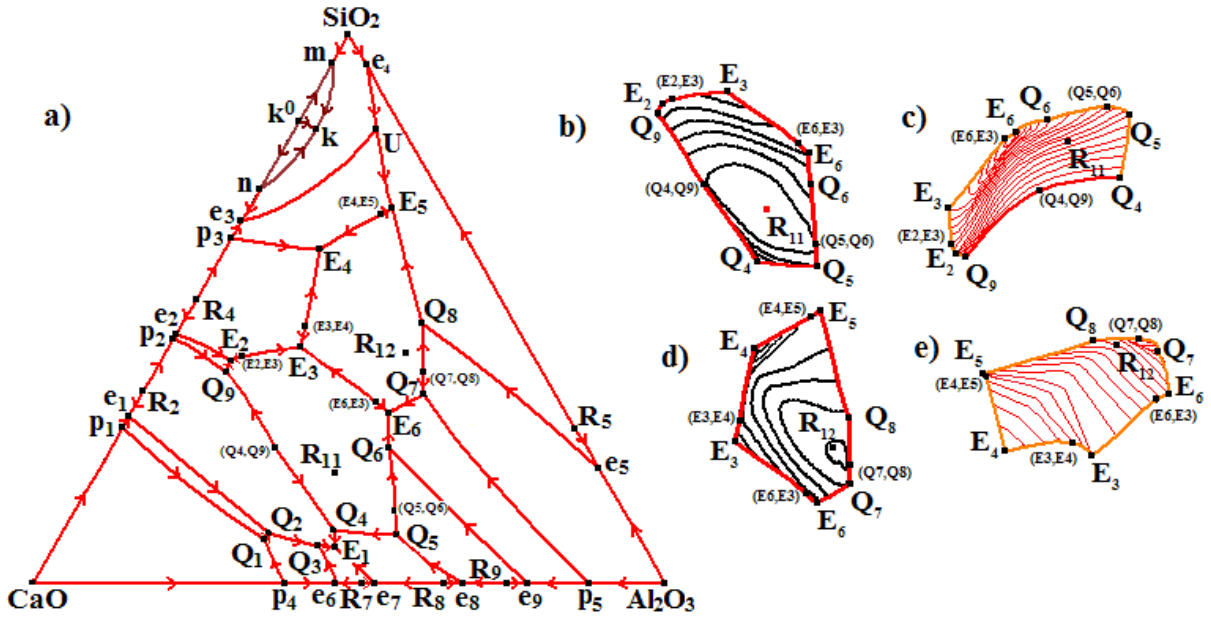

Figure 1. XY projection of liquidus surfaces (a), isolines and 3D models of liquidus surfaces R_{11} (b-c) and R_{12} (d-e)

Let's consider the analysis technology of concentration fields using liquidus field Al_2O_3 ($Al_2O_3p_5Q_7(Q_7,Q_8)Q_8e_5$) as an example. At the projection of considered fragment of phase diagram is divided into 46 concentration fields, including 12 two-dimensional, 23 one-dimensional and 11 zero-dimensional fields (fig. 2a). The diagrams of vertical mass balance have been calculated for each concentration field. They permit to obtain the lists of intersected phase regions and the crystallization schemes for given mass center over the entire temperature range. As a result, it was revealed that two fields coincide with adjacent fields of higher dimension by crystallization stage and microconstituents: R_{10}-$2 \in R_{10}$-2-3 and $2 \in$ 2-3. Furthermore, three concentration fields coincide with adjacent fields by microconstituents, but differ by the crystallization stages: Q_7-$5 \in$ 4-Q_7-5, 6-$Q_8 \in Q_8$-6-7, Q_8-$8 \in Q_8$-7-8.

Using the diagram of vertical mass balance we can consider in more detail the concentration fields having same microconstituents, but different by crystallization stages, e.g. for fields Q_8-8 and Q_8-7-8. The mass center $G_1(0.105; 0.375; 0.52)$ given in two-dimensional field Q_8-7-8 intersects four-phase region (L+C, L+C+R_5, L+R_5+R_{12}, B+R_5+R_{12}) and two horizontal complexes at the temperatures of invariant points (Q_8 and E_5) (fig. 2b).

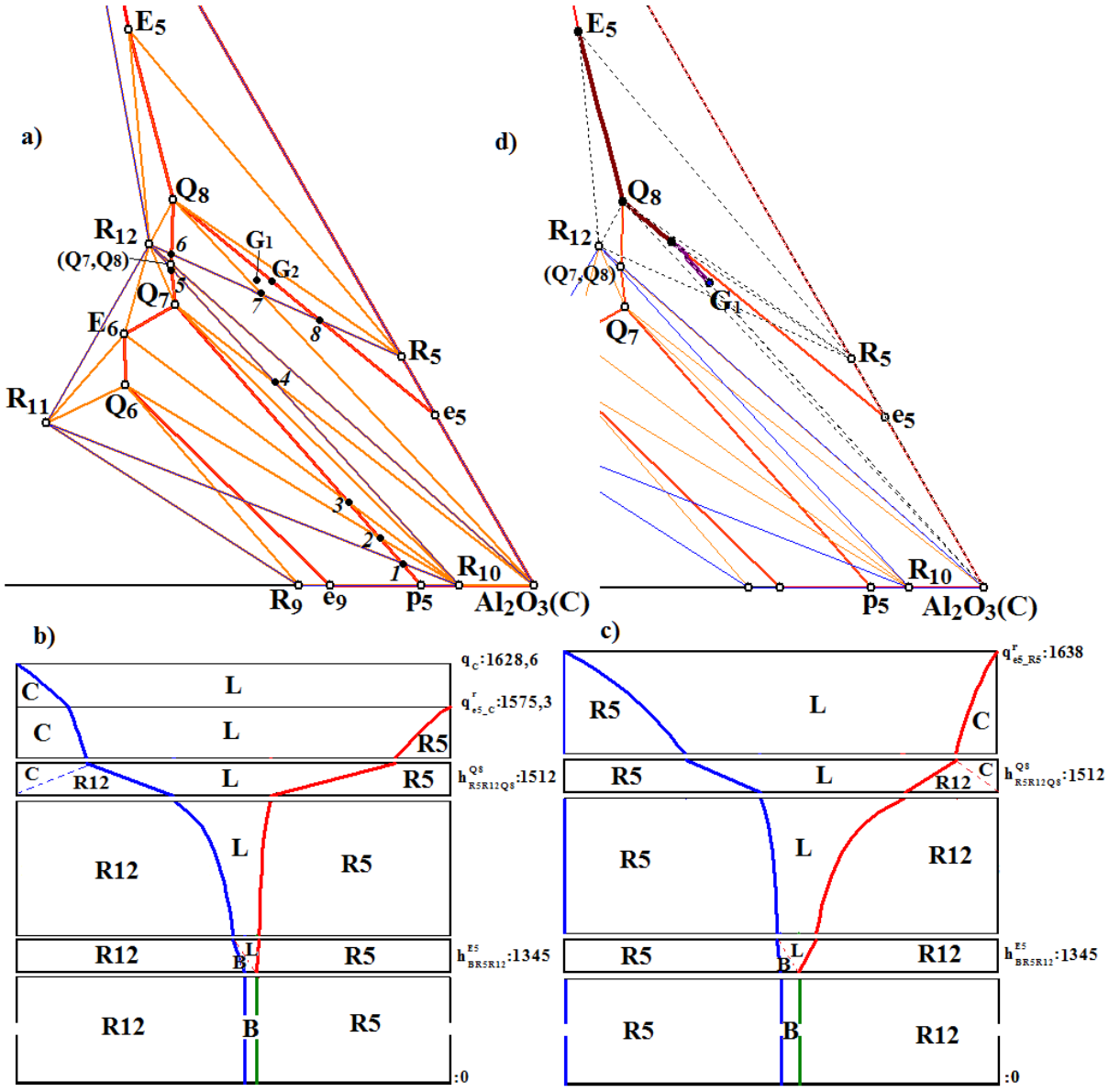

Figure 2. Fragment of projection of T-x-y diagram with dividing of liquidus field Al_2O_3 on the concentration field (a), diagrams of vertical mass balance for compositions G_1 (b) and G_2 (c), crystallization path for G_1 (d)

As can be seen from the diagram of vertical mass balance, there are the increasing of phase portion C and decreasing of phase L in two-phase regions L+C. So, the reaction of primary crystallization takes place $L^1 \rightarrow C^1$. Further, the mass center falls into three-phase L+C+R_5, with the increasing of phases C and R_5, while the phase L continues to decrease. It corresponds the monovariant eutectic reaction $L^e \rightarrow C^{e(R5)} + R_5^{e(C)}$. Next, the invariant quasi-peritectic reaction $L^{Q8} + C^{1,e} \rightarrow R_5^{Q8} + R_{12}^{Q8}$ take place on the horizontal complexed at point Q_8. As a result of this reaction the crystals C is fully expended. In similar way, the postperitectic secondary eutectic reaction $L^{ep} \rightarrow R_5^{ep(R12)} + R_{12}^{ep(R5)}$ occurs in the three-phase region L+R_5+R_{12}. The phase L is fully disappeared as the result of invariant eutectic reaction $L^{E5} \rightarrow B^{E5} + R_5^{E5} + R_{12}^{E5}$ on the plane at the temperature of ternary eutectic points E_5. Below the horizontal complex, the composition gets to the solid-phase region B+R_5+R_{12}. Since the crystals phase

C^1 and C^e are fully expended at the invariant quasi-peritectic reaction, therefore they are not included in the final set of microconstituents. Thus two-dimensional field Q_8-7-8 is characterized by the following set of microconstituents: $R_5^{e5(C)}$, R_5^{Q8}, R_{12}^{Q8}, $R_5^{ep(R12)}$, $R_{12}^{ep(R5)}$, B^{E5}, R_5^{E5}, R_{12}^{E5}. As the field Q_8-8 is a part of monovariant liquidus line e_5Q_8, then it hasn't the reaction of primary crystallization $L^1 \rightarrow C^1$. The mass center G_2(0.092; 0.376; 0.532) for this field at once gets into three-phase region $L+C+R_5$ (fig. 2c). So, one-dimensional field Q_8-8 has shorter crystallization scheme, but coincides with adjacent two-dimensional field Q_8-7-8 by set of microconstituents.

Figure 2d show the crystallization path for mass center G_1 given in considered two-dimensional field Q_8-7-8. The melt G_1 moves along the segment C-G_1 to the liquidus line e_5Q_8 at the passing through two-phase region L+C. Next it falls into three-phase region $L+C+R_5$ and the composition of melt moves along the fragment of liquidus line e_5Q_8 to point Q_8. Then melt shifts along the monovariant liquidus line Q_8E_5 to point E_5 at the going through three-phase region $L+R_5+R_{12}$. The reaction $L^{E5} \rightarrow B^{E5}+R_5^{E5}+R_{12}^{E5}$ is finished on horizontal complex $B_2R_5R_{12}$ and below there are only solid crystals B, R_5,R_{12}.

3. Model of T-x-y diagrams of system $MgO-SiO_2-Al_2O_3$

The system $MgO-SiO_2-Al_2O_3$ has a more simple geometric structure. It is includes three binary congruently melting compounds ($R_1=2MgO{\cdot}SiO_2$, $R_3=3Al_2O_3{\cdot}2SiO_2$, $R_4=MgO{\cdot}Al_2O_3$), one binary ($R_2=MgO{\cdot}SiO_2$) and two ternary ($R_5=4MgO{\cdot}5Al_2O_3{\cdot}2SiO_2$, $R_6=2MgO{\cdot}2Al_2O_3{\cdot}5SiO_2$) incongruently melting compounds. Systems $MgO-SiO_2-Al_2O_3$ is characterized by 11 invariant transformations: three eutectic 3 eutectic (E_{1-3}), one peritectic (P), five quasiperitectic (Q_{1-5}) transformations and 2 four-phase regroupings of phases with polymorphous modification of silicon oxide (cristobalite and tridymite) (fig. 3).

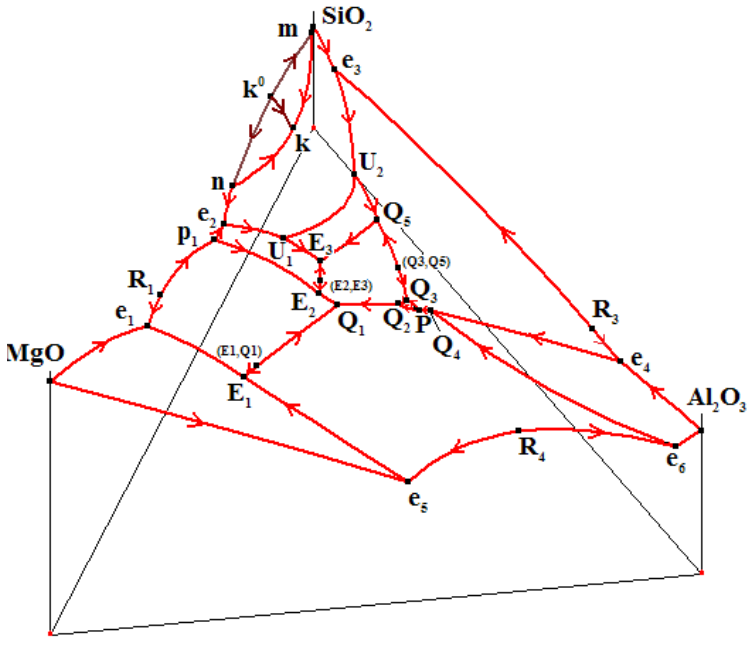

Figure 3. 3D model of liquidus surfaces of system $MgO-SiO_2-Al_2O_3$

Model of T-x-y diagram includes liquid immiscibility surface, 10 liquidus surfaces, 78 ruled surfaces, 11 horizontal complexes at the temperatures of invariant points, 21 two-phase regions and 29 three-phase regions (fig. 4).

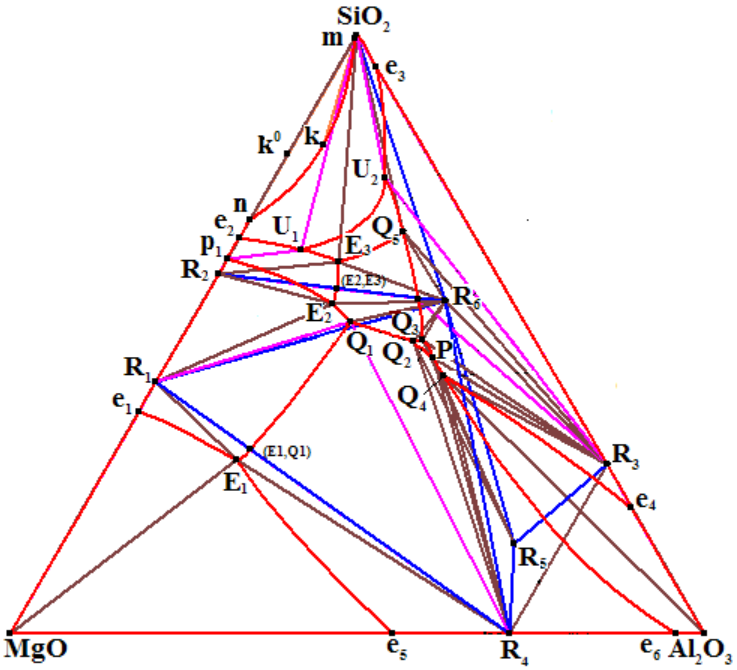

Figure 4. Projection of T-x-y diagram of system $MgO\text{-}SiO_2\text{-}Al_2O_3$

Ternary points U_1 and U_2 arrange at the same temperature, and the points $B1_{U1}$, $B2_{U1}$, $B1_{U2}$, $B2_{U2}$ coincident into one point on the prism edge. Therefore, the horizontal planes corresponding the four-phase phase regroupings of phases $L_{U1}+B_1 \leftrightarrows R_2+B_2$ and $L_{U2}+B_1 \leftrightarrows R_3+B_2$ have degenerated structure $U_1\text{-}R2_{U1}\text{-}B1_{U1}(B2_{U1})$ and $U_2\text{-}R3_{U2}\text{-}B1_{U2}(B2_{U2})$, correspondingly. Phase region $L+B_1+B_2$ degenerate into the plane and the corresponding monovariant peritectic reaction $L^p+B_1 \rightarrow B_2{}^p$ occurs at one temperature.

Projection T-x-y diagram is divided into 100 two-dimensional, 170 one- dimensional and 71 zero-dimensional concentration field. As an example, we carry out an analysis of concentration fields located below the immiscibility surface ($nkmk^0$) and the adjacent liquidus field of cristobalite ($e_2U_1U_2e_3$) (fig. 5a). At projection, they are divided into 9 two-dimensional, 16 one-dimensional and 7 zero-dimensional concentration fields. At that four field coincide by crystallization stages and microconstituents: $B\text{-}3 \in B\text{-}3\text{-}4$; $B\text{-}1 \in e_2\text{-}n\text{-}k\text{-}1\text{-}B\text{-}U_1$; $k \in nk$; $1 \in B\text{-}1$. Additionally 11 concentration fields differ by crystallization stages, by coincide microconstituents ($B\text{-}m\text{-}1$, $e_2\text{-}U_1$, $n\text{-}k$, $m\text{-}1$, $k\text{-}1$ (inside immiscibility surface), $k\text{-}1$ (on the contour of immiscibility surface)$\in e_2\text{-}n\text{-}k\text{-}1\text{-}B\text{-}U_1$; $U_2\text{-}3 \in B\text{-}U_2\text{-}3$, $e_3\text{-}4 \in B\text{-}e_3\text{-}4$, $4 \in B\text{-}4$, $3 \in B\text{-}3$, $U_1 \in B\text{-}U_1$).

A large quantity of concentration fields with coinciding microconstituents due to the presence of phase regions with liquids immiscibility and two polymorphous modifications of component SiO_2. Processes occurring in the phase regions L_1+L_1, $L_1+L_1+B_1$, $L+B_1$ not influence on the final set of microconstituents, because the products of reactions for these fields fully expended. Let's consider two-dimensional field $B\text{-}U_1\text{-}2$ as an example. The mass center G (0.1; 0.8; 0.1) given in this field intersects five 5 phase regions $L+B_1$, $L+B_1+B_2$, $L+B_2$, $L+B_2+R_2$, $B_2+R_2+R_6$ (Fig. 5b) with the following phase reactions $L^1 \rightarrow B_1{}^1$, $L^p+B_1 \rightarrow B_2{}^p$, $L^{1p} \rightarrow B_2{}^{1p}$, $L^{ep} \rightarrow B_2{}^{R2,ep}+R_2{}^{B2,ep}$, $L^{E3} \rightarrow B_2{}^{E3}+R_2{}^{E3}+R_6{}^{E3}$ (^{1} – primary crystallization; ^{p} – monovariant peritectic reaction; ^{1p} – postperitectic primary crystallization; ^{ep} – post-peritectic monovariant crystallization; ^{E} – invariant eutectic crystallization). The crystals B_1 are fully disappeared as the result of postperitectic primary reaction $L^{1p} \rightarrow B_2{}^{1p}$ and they are not included in the set of microconstituents. Thus, the field $B\text{-}U_1\text{-}2$ is characterized by the following microconstituents: $B_2{}^p$, $B_2{}^{1p}$, $B_2{}^{R2,ep}$, $R_2{}^{B2,ep}$, $B_2{}^{E3}$, $R_2{}^{E3}$, $R_6{}^{E3}$.

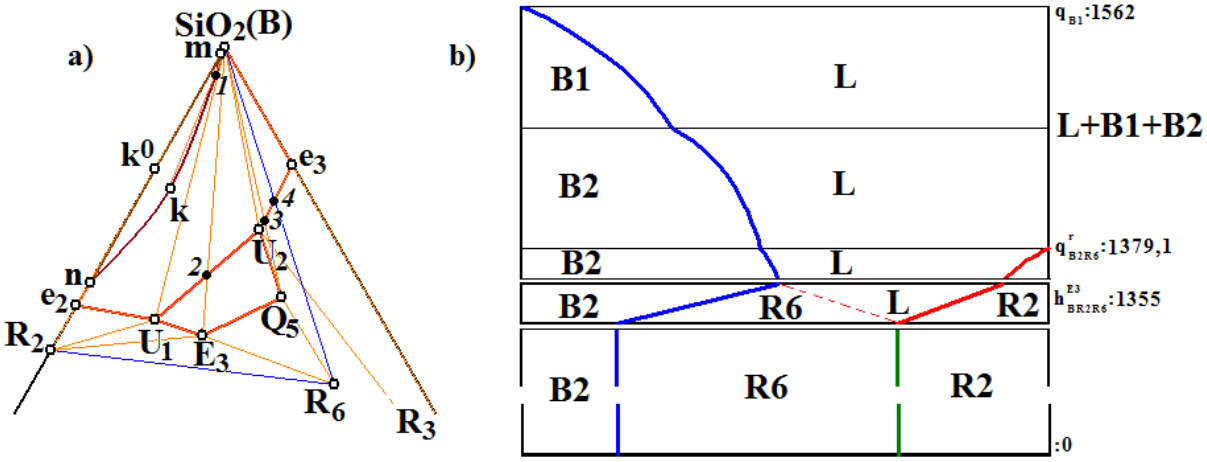

Figure 5. Fragment of phase diagram of system MgO-SiO_2-Al_2O_3 with the dividing into concentration fields

4. Summary

Analysis of two, one and zero-dimensional concentration fields for obtaining the data for the crystallization stages and microconstituents are shown based on the computer models [14] of systems CaO-SiO_2-Al_2O_3 and MgO-SiO_2-Al_2O_3.

Acknowledgement

This work has been performed under the program of fundamental research SB RAS (project 0336-2014-0003) and was partially supported by the Russian Foundation for Basic Research (projects 14-08-00453, 15-43-04304).

References

[1] Lutsyk V I, Vorob'eva V P and Zelenaya A E 2015 *Solid State Phenomena* **230** 51
[2] Lutsyk V I, Zyryanov A M and Zelenaya A E 2008 *Rus. J. Inorg. Chem.* **53** 794
[3] Lutsyk V I, Zelenaya A E and Zyryanov 2009 *Crystallogr. Rep.* **54** 1300
[4] Lutsyk V and Zelenaya 2013 *Journal of Silicate Based and Composite Materials* **2** 34
[5] Lutsyk V I, Zelenaya A E and Zyryanov A M 2008 *Journal of Materials, Methods & Technologies, International Science Publications* **2** 176
[6] Taylor H F W 1997 *Cement Chemistry* (London: Thomas Telford)
[7] Lea F 1998 *Lea's Chemistry of Cement and Concrete* (London: Elsevier Ltd)
[8] Zharikov V A 2005 *Basis of physical geochemistry* (Moscow.: Nauka) (In Russian)
[9] Zavarickij A N and Sobolev V S 1961 *Physico-chemical basis of petrography of eruptive rocks* (Moscow: GOSGEOLTEHIZDAT) (In Russian)
[10] Toropov N A, Bazarkovsky V P, Lapin V V et al. 1972 *Diagrams of Silicate Systems. Vol 3. Ternary Silicate Systems* (Leningrad: Nauka) (In Russian)
[11] Lutsyk V I, Zelenaya A E and Savinov V V 2011 *IOP Conference Series: Materials Science and Engineering* **18** 112005
[12] Lutsyk V and Zelenaya A 2013 *Solid State Phenomena* **200** 73
[13] Lutsyk V I, Zelenaya A E and Savinov V V 2012 *Crystallogr. Rep.* **57** 943
[14] Lutsyk V, Zelena A. 2013 *Építőanyag-JSBCM* ***65*** *34* http://dx.doi.org/10.14382/epitoanyag-jsbcm.2013.7